JOURNAL OF OPTOELECTRONICS AND ADVANCED MATERIALS Vol. 15, No. 7-8, July - August 2013, p. 615 - 620

Theoretical approach for type-i semiconductor spherical core-shell quantum dots heterostructure with wide band gaps

T. O. CHECHE[a*], V. BARNA[a], I. STAMATIN[a,b]
[a] *University of Bucharest ,Faculty of Physics, Bucharest – Magurele 077125, Romania*
[b] *University of Bucharest ,Faculty of Physics, 3Nano-SAE Res Centre, Bucharest-Magurele 077125, Romania*

Within the effective mass approximation a one-band model is adopted to obtain the energy structure and the oscillator strength of type-I semiconductor spherical core-shell quantum dot heterostructure. The core-shell lattice mismatch strain is modeled by the elastic continuum approach. The model is applied to CdTe/ZnSe, a wide band gap type-I heterostructure. We obtain a fair agreement between the simulated absorption spectrum and the available experimental results.

(Received February 17, 2013, accepted July 11, 2013)

Keywords: Quantum Dots, Core-Shell, Absorption Spectrum

1. Introduction

The discreteness of the optical spectra of the semiconductor quantum dots (QDs) is the most significant characteristic of these materials, which makes them very attractive from the perspective of developing novel optical and electronic devices. Size, shape and compounds forming QDs are parameters that confer a high level of controllability of the physical properties of such nanostructures. The colloidal core-shell semiconductor QDs have been chemically synthesized [1-3] with reproducible and controllable size and shape and low fabrication cost. Their high quantum yields and the possibility of tuning the band gap by the shell thickness have attracted many research groups. Both type-I and II core-shell QDs have been shown to have useful application, for example in obtaining sensors [4] or solar cells devices [5].

Theoretically, several approaches have been used to calculate the electronic structures of semiconductor QDs, for example, the tight-binding method [6], the effective bond-orbital model [7], the valence force field model [8] or first-principles calculations [9], the envelope-function methods as the effective mass approximation [10] or multi-band approach [11, 12]. Each of these methods has some limitations either in the accuracy of the predicted electronic structures or the computation cost. Thus, a simple yet realistic model for describing the energy structures will be highly desired for the design of the core-shell QDs for device applications.

In Ref. [13] a simple one-band model within the effective mass approximation, able to describe the energy structure and some optical properties of the core-shell QD heterostructures is introduced. The model is valid for wide band gap semiconductor heterostructures (in this case the mixing of the conduction band (CB) and valence band (VB) is weak) and small QDs (in which it was found that the heavy hole-light hole admixture is less pronounced [12, 14, 15]). The strain induced by the lattice mismatch at the interface is taken into account within an elastic continuum model. An ideal defect–free crystal structure is assumed (to avoid the growth defects, the shell thickness should be of only several monolayers). As the QD model has spherical symmetry, the piezoelectric effect is expected to be less significant [16], and consequently it is neglected. In Ref. [13] the type-II semiconductor heterostructure is analyzed. In the present work, based on the model introduced in Ref. [13], we consider the type-I semiconductor spherical core-shell QDs heterostructures. A comparison between some properties of the type I and II semiconductor spherical core-shell QD heterostructures predicted by the model is made. To make the presentation self-consistent, we remind in this work the main characteristics of the model introduced in Ref. [13].

The structure of the paper is as follows. In Sec. 2, the theoretical model used to obtain the energy structure of type-I semiconductor spherical core-shell quantum dots heterostructure is described. In Sec. 3, the model is applied to CdTe/ZnSe, which is a wide band gap type-I heterostructure. The validity of the approximations used, and the comparison of the predicted and experimental absorption spectra are discussed in this section. Conclusions are given in Sec. 4.

2. One-band model for core-shell semiconductor quantum dots

To obtain the energy structure within the one-band model one needs to know the bulk band-offset of the hetersotructure and the effective masses of the carriers. According to the *model-solid theory* developed by Van de Walle [17], both VB and CB are shifted by the hydrostatic

deformation potential and, in addition, by the spin-orbit coupling in the case of the VB. The value of the band edge is given by [17]

$$E_v = E_v^0 + \frac{\Delta}{3} + a_v \frac{\Delta\Omega}{\Omega} \tag{1a}$$

$$E_c = E_c^0 + a_c \frac{\Delta\Omega}{\Omega} \tag{1b}$$

where v (c) holds for VB (CB), E_v^0 and E_c^0 denote the unstrained values of the band edges, Δ is the spin-orbit splitting, a_v and a_c are the corresponding hydrostatic deformation potentials, $\Delta\Omega/\Omega = \varepsilon_{hyd}$ is the fractional volume change due to the hydrostatic strain.

For CdTe/ZnSe core-shell QDs, the type-I heterostructure we discuss in this work, we draw in Fig. 1 the schematic band lineups corresponding to the strained case (notations are in accordance with those from Eqs. (1)). On the external surface of the

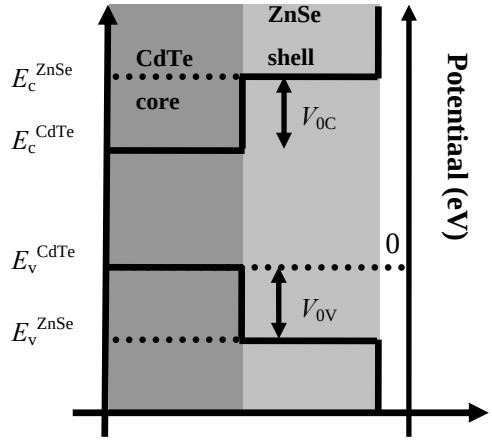

Fig. 1 Schematic band lineups for CdTe/ZnSe core-shell QD in presence of strain. The notations of the energies are in accordance with Eq. (1).

shell, the potential is approximated by a hard wall. According to Fig. 1, we consider the following spherical square-well potentials as functions of r:

i) for electrons:

$$V(r) = \begin{cases} 0, \text{ if } 0 \le r < r_0 \\ V_{0C}, \text{ if } r_0 \le r < R \\ \infty, \text{ if } r \ge R \end{cases}; \tag{2a}$$

ii) for holes:

$$V(r) = \begin{cases} 0, \text{ if } 0 \le r < r_0 \\ V_{0V}, \text{ if } r_0 \le r < R \\ \infty, \text{ if } r \ge R \end{cases}; \tag{2b}$$

with $V_{0C} = E_v^{ZnSe} - E_v^{CdTe} > 0$, $V_{0V} = -E_v^{ZnSe} > 0$. In spherical coordinates the Schrödinger equation:

$$\left[\frac{-\hbar^2}{2m^*(r)}\frac{1}{r}\frac{\partial^2}{\partial r^2}r + \frac{1}{2m^*(r)r^2}\mathbf{L} + V(r)\right]\psi(\mathbf{r}) = E\psi(\mathbf{r})$$

where $\mathbf{L}$ is the orbital angular momentum and $m^*(r)$ is the position-dependent effective mass. Following the standard procedure, we look for solutions that are products of radial part $R_l(r)$ and spherical harmonic $Y_{lm}(\theta,\varphi)$ functions. Taking into account the commutation relations between the above Hamiltonian and the orbital angular momentum one obtains the single -particle radial Schrödinger equation

$$\begin{aligned} &\frac{-\hbar^2}{2m^*(r)}\frac{1}{r}\frac{d^2}{dr^2}\left[rR_l(r)\right] + \frac{l(l+1)\hbar^2}{2m^*(r)r^2}R_l(r) \\ &= \left[E - V(r)\right]R_l(r) \end{aligned}, \tag{3a}$$

For Eq. (3a) we search solution by using the change of variable, $\rho = k_i r$, where $k_i^2 = \mp 2m_i(E - V_i) > 0$ if $E \gtrless V_i$ (with the notations, $m_i = m_{1,2}^{e,h}$ for the effective mass of the electron (e) or hole (h) in the core (i=1) or shell (i=2), and V_i for the values of the piecewise-constant potential in region i, that is, $V_i = 0$ or V_{0V} or V_{0C}), Eq. (3a) reduces to the Bessel differential equation

$$\begin{aligned} &\rho^2\frac{d^2v_l(\rho)}{d\rho^2} + 2\rho\frac{dv_l(\rho)}{d\rho} - l(l+1)v_l(\rho) \\ &\mp \rho^2 v_l(\rho) = 0 \end{aligned}, \tag{3b}$$

and consequently, the general solution of Eq. (3a) is of the form $R_l(r) = v_l(k_i r)$. In Eq. (3b) the sign of the last term is positive for $E > V_i$ and negative for $E < V_i$. The solutions of Eq. (3b) are linear combinations of spherical Bessel or modified spherical Bessel functions, namely: $v_l(\rho) = A_l j_l(\rho) + B_l y_l(\rho)$ if $E > V_i$ or $v_l(\rho) = A_l i_l(\rho) + B_l k_l(\rho)$ if $E < V_i$, where $j_l(\rho)$, $y_l(\rho)$ are the spherical Bessel functions of the first and second kind, and $i_l(\rho)$, $k_l(\rho)$ are the modified spherical Bessel functions of the first and second kind, respectively. The solutions should be regular and consequently we disregard in the linear combinations of solutions the functions infinite in origin. Thus, solutions should be of the following form.

Electronic states

For $0 \le r \le r_0$:

$$R_l^{(1e)}(r) = A_l^e j_l(k_1^e r). \tag{4a}$$

For $r_0 \le r \le R$:

$$E < V_{0C},\ R_l^{(2e)}(r) = \left[B_l^e k_l(k_2^e r) + F_l^e i_l(k_2^e r)\right], \tag{4b}$$

$$E > V_{0C},\ R_l^{(3e)}(r) = \left[C_l^e j_l(k_3^e r) + D_l^e y_l(k_3^e r)\right]. \tag{4c}$$

In Eqs. (4), $k_1^e = \sqrt{2m_1^h E}\,/\hbar$, $k_2^e = \sqrt{2m_2^h(-E + V_{0C})}\,/\hbar$, $k_3^e = \sqrt{2m_2^h(E - V_{0C})}\,/\hbar$, and A_l^e, B_l^e, F_l^e, C_l^e, D_l^e are orthonormalization constants.

The explicit expressions of the wave functions are obtained by imposing the continuity of the wave function and probability current, and the vanishing of the wave function outside the QD. Thus, for the case $E < V_{0C}$:

$$\begin{cases} R_l^{(1e)}(r_0) = R_l^{(2e)}(r_0) \\ \dfrac{1}{m_1^e}\dfrac{dR_l^{(1e)}(r)}{dr}\bigg|_{r_0} = \dfrac{1}{m_2^e}\dfrac{dR_l^{(2e)}(r)}{dr}\bigg|_{r_0} \\ R_l^{(2e)}(R) = 0 \end{cases}, \tag{5a}$$

Then, the energy is obtained by solving the transcendental equation

$$\frac{m_2^e}{m_1^e}\frac{j_l'(k_1^e r_0)}{j_l(k_1^e r_0)} = \frac{-k_l'(k_2^e r_0) + k_l(k_2^e R) i_l'(k_2^e r_0)/i_l(k_2^e R)}{-k_l(k_2^e r_0) + k_l(k_2^e R) i_l(k_2^e r_0)/i_l(k_2^e R)} \tag{5b}$$

For the case $E > V_{0C}$ the equations expressing the boundary conditions and solutions are similar with those from Eq. (5), by replacing $R_l^{(2e)}$ by $R_l^{(3e)}$, k_2^e by k_3^e, i_l by y_l, and k_l by j_l.

For hole states the equations expressing the boundary conditions and solutions are similar with those from Eqs. (4) and (5), by replacing the index *e* by *h*. The conditions $R_l^{(2e,3e)}(R) = 0$, $R_l^{(2h,3h)}(R) = 0$ impose the wave functions have a node on the external surface of the shell.

The solutions for the energy and normalizations constants of Eqs. (5) implies knowing of the strain. For the implementation of strain effect on the VB to a II-VI zinc blende heterostructure, we may apply Eq. (5) (written for holes) to the heavy and light holes separately, by using the same V_{0V}, but different effective masses [13]. In the calculation, we consider the spherical part of the heavy-hole mass (m^{hh}) and light-hole masses (m^{lh}) assumed by the parabolic dispersion of the one-band model [13],

$$m^{hh,(lh)} = \frac{m_0}{\gamma_1}\left[1 - (+)\frac{6\gamma_3 + 4\gamma_2}{5\gamma_1}\right] \tag{6}$$

Finally, by superposing the two sets of hole states, we obtain the approximate VB energy structure.

For the concrete band lineups, we need to know the hydrostatic strain. For the core-shell geometry, within the continuum elasticity approach by imposing the inner and outer material shrink–fit condition to the radial displacement introduced by the strain, we obtain [13]:

$$\varepsilon_{1hyd} = 2\varepsilon_0\left[1 - \left(\frac{r_0}{R}\right)^3\right]\frac{1-2\nu_1}{1-\nu_1}, \tag{7a}$$

$$\varepsilon_{2hyd} = -\frac{2\varepsilon_0}{3}\left(\frac{r_0}{R}\right)^3\frac{1-2\nu_2}{1-\nu_2}, \tag{7b}$$

where the subscript 1(2) holds for the core(shell), ε_0 is the relative mismatch, and $\nu_{1,(2)}$ is the Poisson ratio of the core (shell) material. For CdTe/ZnSe core-shell QD, the case we analyze in Sec. 3, the lattice constant of CdTe, a_1, is larger than the lattice constant of ZnSe, a_2, and one obtains the strain is compressive for the core and tensile for the shell. Quantitatively, the relative lattice mismatch $\varepsilon_0 = (a_2 - a_1)/a_1$ is negative and according to Eqs. (7), $\varepsilon_{1hyd} < 0$ (compression), and $\varepsilon_{2hyd} > 0$ (dilation).

3. Application to CdTe/ZnSe core-shell quantum dots

The band lineups in presence of strain are obtained by using the model-solid theory of Van de Walle [17] as follows. For the bulk (unstrained) band-offset, we consider the gap energies [17], $E_{g0}^{\mathrm{CdTe}} = 1.59\mathrm{eV}$, $E_{g0}^{\mathrm{ZnSe}} = 2.83$, $a_1 = 0.648\mathrm{nm}$, $a_2 = 0.566\mathrm{nm}$, $v_1 = 0.410\mathrm{nm}$, $v_2 = 0.375\mathrm{nm}$, $\Delta_{\mathrm{CdTe}} = 0.93\mathrm{eV}$, $\Delta_{\mathrm{ZnSe}} = 0.43\mathrm{eV}$, $E_{v0}^{\mathrm{CdTe}} = -7.07\mathrm{eV}$, $E_{v0}^{\mathrm{ZnSe}} = -8.37\mathrm{eV}$, $E_{c0}^{\mathrm{CdTe}} = -5.17\mathrm{eV}$, and $E_{c0}^{\mathrm{ZnSe}} = -5.40\mathrm{eV}$. With these bulk values of the energies and by using Eqs. (1) and (7) (with the large relative lattice mismatch of $\varepsilon_0 = -0.128$), we find the band lineups in presence of strain as function of R and r_0 as shown in Fig. 2. One obtains that the strain induces enlargement (shrinkage) of the band gap for CdTe (ZnSe), and the band gaps, $E_g^{\mathrm{CdTe}} = E_c^{\mathrm{CdTe}} - E_v^{\mathrm{CdTe}}$, $E_g^{\mathrm{ZnSe}} = E_c^{\mathrm{ZnSe}} - E_v^{\mathrm{ZnSe}}$, increase with the shell thickness, results that are similar (because of the same sign of ε_0) with those reported for ZnTe/ZnSe (type-I heterostructure) spherical core-shell quantum dots [13]. The band lineups with the strain taken into account are in the intervals, $V_{0C} = 0.639 \div 0.554\mathrm{eV}$, $V_{0V} = 1.316 \div 1.408\mathrm{eV}$ for $R = 1.9 \div 3.6\mathrm{nm}$.

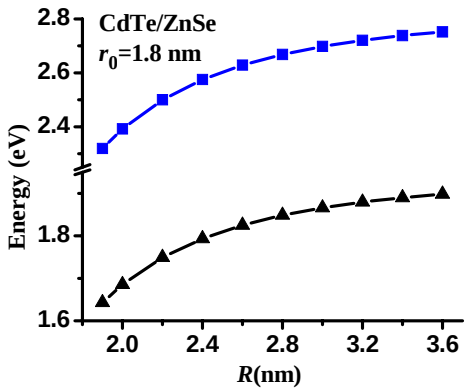

Fig.2. Gap energies of CdTe/ZnSe core-shell QDs in the presence of lattice mismatch strain vs. core+shell radius R, with the core radius r_0=1.8 nm. The legend: ■ E_g^{CdTe} ▲ E_g^{ZnSe}.

Then, with the values of the Luttinger parameters from Lawaetz [18], $\gamma_1^{\mathrm{CdTe}} = 5.29$, $\gamma_2^{\mathrm{CdTe}} = 1.89$, $\gamma_3^{\mathrm{CdTe}} = 2.46$, $\gamma_1^{\mathrm{ZnSe}} = 3.77$, $\gamma_2^{\mathrm{ZnSe}} = 1.24$, $\gamma_3^{\mathrm{ZnSe}} = 1.67$ the spherically averaged hole effective masses according to Eq. (7) are $m_{\mathrm{CdTe}}^{hh} = 1.21m_0$, $m_{\mathrm{CdTe}}^{lh} = 0.10m_0$, $m_{\mathrm{ZnSe}}^{hh} = 1.29m_0$, $m_{\mathrm{ZnSe}}^{lh} = 0.15m_0$. For electrons, we consider the effective masses, $m_{\mathrm{CdTe}} = 0.11m_0$, and $m_{\mathrm{ZnSe}} = 0.21m_0$ [19].

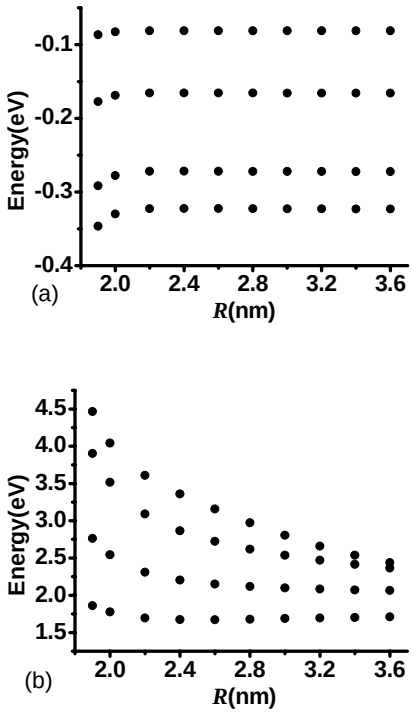

Fig. 3 Energy levels of: (a) holes; (b) electrons for CdTe/ZnSe core-shell QDs vs. core+shell radius R, with the core radius $r_0 = 1.8\mathrm{nm}$.

The energy structure is shown in Fig. 3 for the first four levels for both electrons and (heavy) holes states. With Eq. (5), when comparing the energies values obtained with heavy and light holes, we obtain the first four hole states are heavy hole states. The hole energies in Fig. 3 remain practically unchanged by the shell thickness as a result of the weak mixing of the hole states of the two compounds (large $V_{0\mathrm{V}}$ of the heterostructure). On the other hand, the electron energy decreases with the shell thickness, which results in decreasing of the lowest energy transition, in accordance with the results regarding the absorption and emission spectra reported by Ref. [20] for such CdTe/ZnSe core-shell QDs. In Fig.4, we present the predictions of our model for the spatial density probabilities (orbitals), $\left|R_{nl}^{(\alpha)}(r)Y_{lm}(\theta,\varphi)\right|^2$, for CdTe/ZnSe core-shell QD with core radius $r_0 = 1.8\mathrm{nm}$, $R = 2.2,\ 3,\ 3.6(\mathrm{nm})$, and axis *z chosen* as quantization axis. The contour corresponds to $\mathrm{Max}\left(\left|\Psi_{nlm}^{h,e}(\mathbf{r})\right|^2\right)\times 0.75$, and the first two rows are for holes and the next for electrons. The figures are denoted according to the following quantum numbers: (a) $n=1,\ l=0,\ m=0$; (b) $n=1,\ l=1,\ m=0$; (c) $n=1,\ l=1,\ m=\pm 1$; (d) $n=1,\ l=2,\ m=0$; (e) $n=1,\ l=2,\ m=\pm 1$; (f) $n=1,\ l=2,\ m=\pm 2$. The orbitals correspond to the first three electron (hole) energy levels in ascending (descending) order from Fig. 3 ((a) to the first, (b) and (c) to the second, and (d)-(f) to the third).

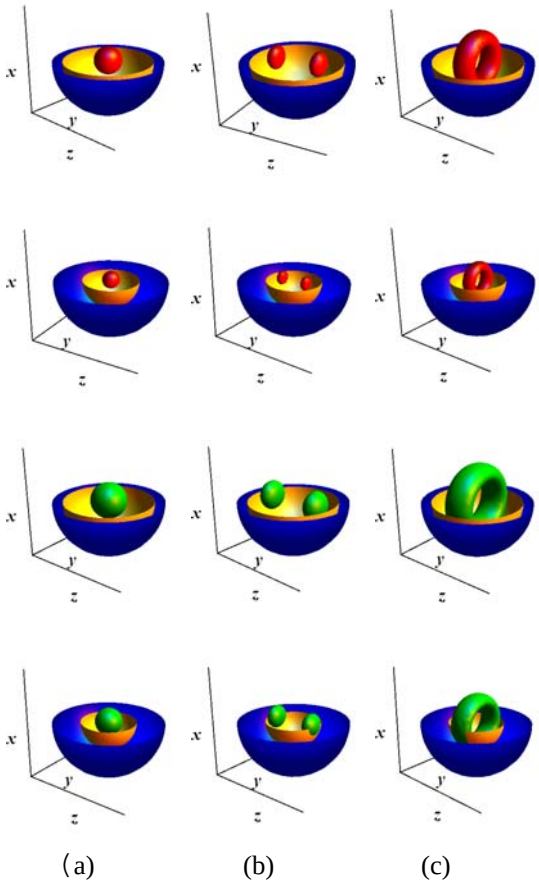

Fig. 4a. Hole (red color) and electron (green color) probability density for the ground and first excited state, see the text.

As the envelope wave functions are similar for electron and holes, the form of the orbitals is also similar, but as effect of the lager hole effective mass, the hole orbitals are shrunk comparatively to the electronic ones. In addition, interesting is the fact that for the excited states the electron is located close to the core-shell interface, a typical characteristic for type-II core-shell-QDs. This indicates that the type-I core-shell QDs could be used in application in solar cells to separate electron-hole pairs, if the electron excited states are those involved in separations. The ground state has spherical symmetry for both electron and hole, which is characteristic for the *s* orbital. The optical spectra can be described by the oscillator strength [13]

$$f_{ij} = \frac{E_P}{\hbar\omega_{ij}} \left| \left\langle \psi^*_{nLm} \middle| \psi_{n'L'm'} \right\rangle \right|^2 , \qquad (8)$$

which characterizes the probability of interband transition between two states, *i* (characterized by the

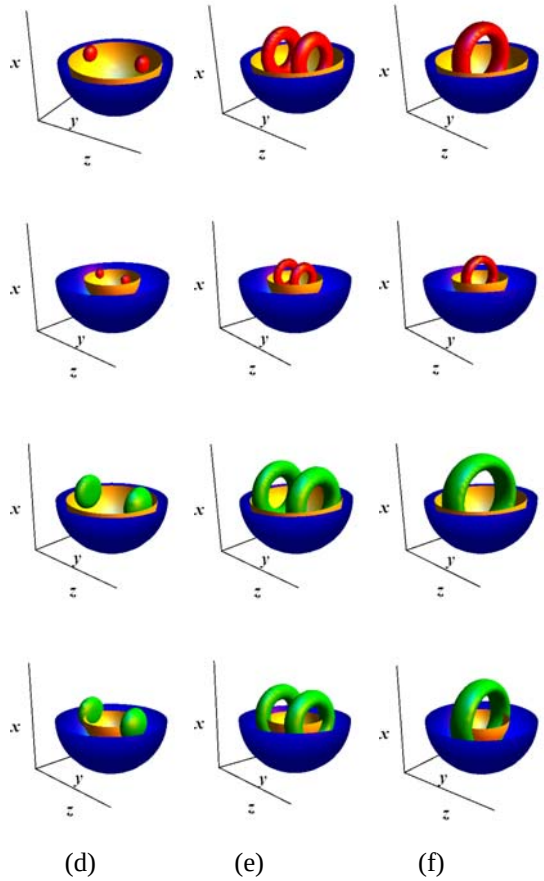

Fig. 4b. Hole (red color) and electron (green color) probability density for the second excited states, see the text.

set of quantum numbers, *n, L, m*) and *j* (characterized by the set of quantum numbers, *n′, L′, m′*); $E_P = 2m_0|P|^2/\hbar^2$ and $P = -i(\hbar/m_0)\langle s|p_x|x\rangle$ is the Kane momentum matrix element. In Fig. 5 we present the influence of the shell thickness on the oscillator strengths obtained from the first four hole and electron states shown in Figs. 3 and 4 (common E_p=18.8eV for both compounds of the core-shell QD [21] is considered). For type-I heterostructures the hole and electron ground envelope wave functions have larger overlap than in the case of the type-II heterostructures, but the oscillator strength is still influenced by the shell thickness. Thus, the oscillator strength decreases with the shell thickness. This is in accordance with the experimental reports that find the shell thickness reduces the quantum yield of CdTe/ZnSe QD [20]. On the other hand, for the exited states, as result of the close location of the electron states to the core-shell interface while the hole states remain localized in the core, the overlaps and consequently the oscillator strengths are smaller. For the excited states, thicker shell leads to a decrease of the oscillator strength too. Comparatively to the type-II heterostructures the oscillator strength is much less influenced by the shell thickness [see Ref. 13]. Thus, less pronounced decrease with the shell thickness of the quantum yield and less efficient separation of the electron-hole pair are expected for type-I comparatively to type-II core-shell QDs. Consequently, according to our model, these two factors, the quantum yield and the electron-hole separation are competing in deciding which kind of herterostructure, type-I or II is more efficient in a potential use of he core-shell QDs in solar cell devices. As another characteristic of the optical absorption, we obtain a red shift of the lowest energy transition, **1** (as denoted in Fig. 5) with the shell thickness, similarly to the experiment [20].

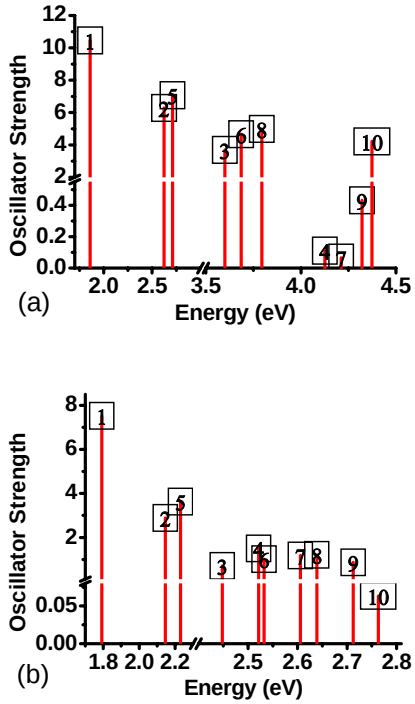

*Fig. 5 The oscillator strength for CdTe/ZnSe core-shell QD with $r_0 = 1.8$nm and a) $R = 2.2$nm , b) $R = 3.6$nm . The labels in the figures correspond to the following transitions: **1** for $1 \leftrightarrow 1$, **2** for $1 \leftrightarrow 2$, **3** for $1 \leftrightarrow 3$, **4** for $1 \leftrightarrow 4$, **5** for $2 \leftrightarrow 2$, etc. The labels 1, 2, 3, 4, represent the four electron (holes) states from Fig. 3 in ascending (descending) order of the energy.*

In Fig. 6, we compare the absorption results obtained in Ref. [20] with our simulated results, for CdTe/ZnSe core-shell QDs with $r_0 = 1.8$nm as function of shell thickness. We assign the lowest energy transition, **1**, active one as shown in Fig. 5 to the main peak recorded in Ref. [20] in absorbance measurements. The experimental data are adapted from the absorbance in Fig. 2 (a) from Ref. [20], by taking the ZnSe monolayer thickness of 2.83Å. Experimentally, obtaining uniformly coated cores with spherical shape for the shell is difficult task, but comparison between frequencies of the absorbed light provides a reasonable fit for the simplicity of the model we used.

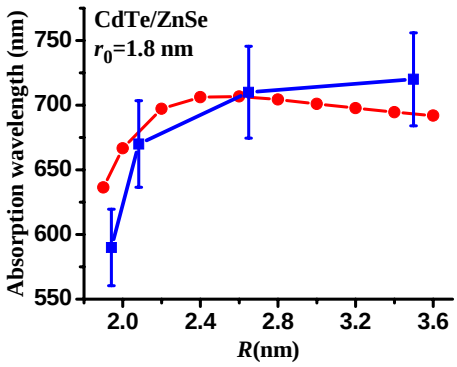

Fig. 6. Absorption wavelength for CdTe/ZnSe core-shell QDs with $r_0 = 1.8\text{nm}$ $r_0 = 2.2\text{nm}$ *as function of the shell thickness. The simulation is obtained for the lowest energy transition corresponding to the transition* ***1*** *(*$1 \leftrightarrow 1$***)*** *in Fig. 5. The error bars of the experimental values are of 5%. The legend:* ■ *- experimental values and* ● *- simulated values.*

4. Conclusions

The one-band model within the effective mass approximation adopted to explain the energy structure of core-shell QDs gives reasonably good results for the wide band gap CdTe/ZnSe heterostructures. The excitonic effect is expected to lead to a correction of the results, but for small QDs (as is the case in our simulation) the Coulombic interaction is negligible with respect to the interlevel energy, and we limit accuracy of predictions to values of approximately 0.1eV [22]. Of particular importance for the correctness of our modeling is using of rather large effective masses obtained within the spherical approach $m^{hh}_{\text{CdTe}} = 1.21m_0$, $m^{hh}_{\text{ZnSe}} = 1.29m_0$. On the other hand, consideration of the strain is necessary for obtaining a reasonable level of accuracy. The elastic continuum model we adopted proves to be an appropriate approach, in accordance with the opinion of the researchers in the field regarding its validity in describing nanostructures. However, using of an atomistic approach for the strain in case of thinner shell would be useful [23] for comparison of the results. Location of the electron close to the core-shell interface for excited sates constitutes a characteristic that could be useful in engineering solar cells with type-I semiconductor QDs heterostructures. As the present theoretical approach was applied with good results to characterize core-shell QDs type-II heterostructures too [13], we think that given its robustness, and satisfactory accuracy level, the approach is very useful for at least preliminary calculations of the optical properties of core-shell QDs of wide band gap, where the band mixing effect is of less importance.

Acknowledgments

This work was supported in part by the grant POSDRU/89/1.5/S/58852, Project ‘‘Postdoctoral programme for training scientific researcher’’ co-financed by the European Social Found within the Sectorial Operational Program Human Resources Development 2007-2013, and the Romanian National Grants TE 225-96/2010 and ID-PCE-2011/3/1007, ID-PCE-2011/64/2011

References

[1] M. Bruchez, M. Moronne, P. Gin, S. Weiss, A.P. Alivisatos, Science **281**, 2013 (1998); W. C. Chan and S. Nie, Science **281**, 2016 (1998).
[2] X. Michalet, F.F. Pinaud, L.A. Bentolila, J.M. Tsay, S. Doose, J.J. Li, G. Sundaresan, A.M. Wu, S.S. Gambhir, S. Weiss, Science **307**, 538 (2005); X. Gao, Y. Cui, R.M. Levenson, L.W. Chung, S. Nie, Nat. Biotechnol. **22**, 969 (2004); W. Cai, D.W. Shin, K. Chen, O. Gheysens, Q. Cao, S.X. Wang, S.S. Gambhir, X. Chen, Nano Lett. **6**, 669 (2006).
[3] L. Shi, B. Hernandez, M. Selke, J. Am. Chem. Soc. **128**, 6278 (2006).
[4] J.U. Sutter, D.J.S. Birch and O.J. Rolinski, Meas. Sci. Technol. ***23,*** *055103 (2012).*
[5] H. Zhu, N. Song, and T. Lian, J. Am. Chem. Soc. **133**, 8762 (2011), and the references therein.
[6] S. Pokrant, K.B. Whaley, Eur. Phys. J. D **6**, 255 (1999).
[7] S.J. Sun, Y.-C. Chang, Phys. Rev. B **62**, 13631 (2000).
[8] L. He, G. Bester, A. Zunger, Phys. Rev. B **70**, 235316 (2004).
[9] J. Li and L. Wang, Appl. Phys. Lett. **84**, 3648 (2004).
[10] D. Schooss, A. Mews, A. Eychmüller, H. Weller, Phys. Rev. B **49**, 17072(1994).
[11] G.A. Baraff and D. Gershoni, Phys. Rev. B **43**, 4011 (1991); D. Gershoni, C.H. Henry, G.A. Baraff, IEEE J. Quantum. Elect. **9**, 2433 (1993).
[12] P.C. Sercel, K. J. Vahala, Phys. Rev. B **42** 3690 (1990).
[13] T.O. Cheche, V. Barna, Y-C. Chang, Superlattice Microst. **60**, 475 (2013).
[14] Y. Rajakararunnayake, R.H. Miles, G.Y. Wu, T.C. McGill, Phys. Rev. B **37**, 10212 (1988).
[15] L.C. Lew Yan Voon, M. Willatzen, The $\mathbf{k}\cdot\mathbf{p}$ Method, Electronic Properties of Semiconductors (Springer-Verlag Berlin Heidelberg 2009) p.282.
[16] J.H. Davies, J. Appl. Phys. **84**,1358 (1998).
[17] C.G. Van de Walle, Phys. Rev. B **39**, 1871 (1989).
[18] P. Lawaetz, Phys. Rev. B 4, 3460 (1971).
[19] Singh J, Physics of Semiconductors and Their Heterostructures (McGraw-Hill, 1993).
[20] A.M. Smith, A.M. Mohs, and S. Nie, Nat Nanotechnol. 4, 56(2009).
[21] C.R. Becker, V. Latussek, A. Pfeuffer-Jeschke, G. Landwehr, L.W. Molenkamp, Phys Rev B. **62**, 2000, 10353(2000).
[22] From L.E. Brus, J. Chem. Phys. **79**, 5566 (1983).
[23] C. Pryor, J. Kim, L. W. Wang, A. J. Williamson, and A. Zunger, J. Appl. Phys. **83**, 2548 (1998).

*Corresponding author: istarom@3nanosae.org